

Simulations of Near Real-time EOP Estimation from a Future VGOS Network

Tobias Nilsson¹, Maria Karbon¹, Benedikt Soja¹, Susanne Glaser², Robert Heinkelmann¹, Harald Schuh^{1,2}

Abstract We describe the Kalman filter implemented in the VieVS@GFZ software which is able to analyze VLBI data in real-time. The filter is tested through simulations of a real-time estimation scenario from a 30 station VGOS network. We obtain a precision of 20–30 μs for polar motion and celestial pole offsets and 1.3 μs for UT1–UTC. The Kalman filter is able to work fully automated and can detect and correct problems like clock breaks automatically.

Keywords VLBI, VGOS, real-time, Kalman filter

1 Introduction

One of the goals of the upcoming VLBI Geodetic Observing System (VGOS) is to reduce the latency between the observations and the availability of the results, e.g., Earth Orientation Parameters (EOP). For the current VLBI system this latency is about two weeks, and the goal of VGOS is to reduce it to less than 24 hours [7]. Ideally, the results should be available in real-time [1]. Achieving this is challenging for all parts of the VLBI processing chain. First of all, the data needs to be sent with e-transfer in real-time from the stations to the correlator. For this it is required that all the stations, and in particular the correlator, are connected to high-speed electronic networks. Then, as

soon as all the data from a scan have arrived at the correlator, the data are correlated in order to produce the VLBI observables, e.g., the group delays. These are then used as input to a VLBI analysis software, where the interesting parameters, like the EOP, are estimated. The possibility of VLBI in near real-time has been demonstrated for one-hour single-baseline sessions, so-called Intensive sessions [2]. However, for VGOS, real-time operation will be more challenging, especially since the data recording rate for VGOS will be 8–16 Gbps. Although the data do not necessarily need to be sent with this speed, since it is planned to also use the time in which the telescopes slew to the next source for the transfer, still a stable connection to the correlator of several Gbps is needed.

In this work we focus on the challenges for the last part of the VLBI processing chain: the VLBI data analysis. This part, just as the other parts, must run completely autonomous and needs to be able to deal with any problem that may occur, e.g., clock breaks. As soon as the observables from a new scan are available from the correlator, a new solution should be calculated in order to get updated estimates for the EOP and other parameters [1]. Thus it seems appropriate to apply a Kalman filter for the parameter estimation. In this work we apply a modified version of the Kalman filter implemented in the VieVS@GFZ software [5, 8]. The implementation is briefly described in Section 2. The software is tested through simulation of a real-time estimation scenario from a 30-station VGOS network. The setup of the simulations is presented in Section 3 and the results in Section 4. Finally, the conclusions are given in Section 5.

1. GFZ German Research Centre for Geosciences, Section 1.1 Space Geodetic Techniques, Telegrafenberg A17, 14473 Potsdam, Germany

2. Technische Universität Berlin, Institute of Geodesy and Geoinformation Science, Straße des 17. Juni 135, 10623 Berlin, Germany

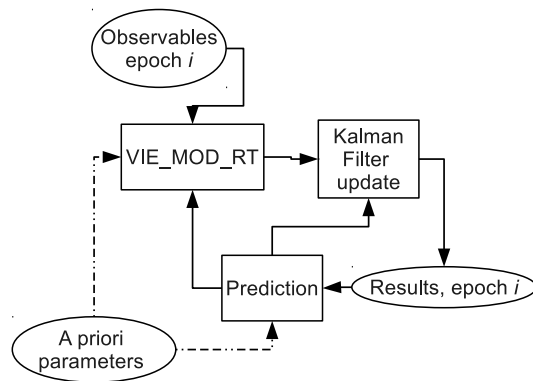


Fig. 1 Flowchart of the real-time VLBI data analysis with VieVS@GFZ.

2 Kalman Filter Implementation

The basic structure of the Kalman filter is shown in Figure 1. Whenever observables from a new scan become available, the theoretical delays and the partial derivatives are calculated using the module VIE_MOD_RT. The a priori parameters needed for these calculations, e.g., the EOP, the station coordinates, and the radio source coordinates, are predicted from the results of the previous epoch, except for the very first epoch where initial guesses of these parameters are used. Then the estimates are updated by the Kalman filter by making an optimal combination of the values predicted from the previous epoch and the observables of the current epoch. For more details, see [5]. For the real-time analysis, the Kalman filter loop only runs forward in time. However, the option also exists to run the filter backwards in time, followed by smoothing where the optimal combination of the forward and backward results is calculated. This will only improve the results at the earlier epochs, not the last one. Hence, this option is only applicable for post-processing.

In the Kalman filter the following parameters are estimated: all five EOP (modeled as integrated random walk processes), station coordinates (highly constrained random walk processes), radio source coordinates (constant offsets), zenith wet delays (random walk), tropospheric gradients (random walk), and clock errors (random walk plus integrated random walk). The datum for the station coordinates is realized by adding No-Net-Rotation (NNR) and No-Net-Translation (NNT) constraints as additional

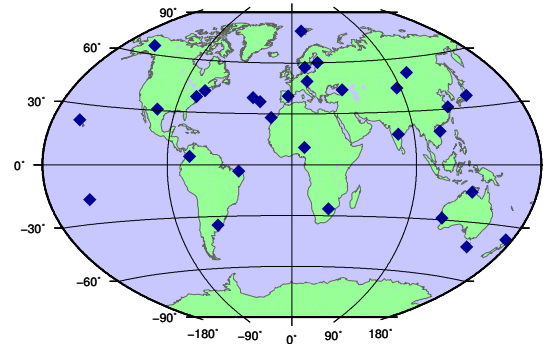


Fig. 2 The 30-station VGOS network used for the simulations.

pseudo-observations. Similarly, the datum for the radio sources is realized by NNR constraints.

3 Simulations

To test the real-time Kalman filter we made simulations. Here we assumed a future observing scenario with a 30-station VGOS network (see Figure 2). For most antennas we assumed a slew rate of $12^\circ/\text{s}$ in azimuth and $6^\circ/\text{s}$ in elevation. The exceptions were existing antennas with different slew rates, i.e., the antennas in Australia, New Zealand, and at the Goddard Geophysical and Astronomical Observatory (GGAO), USA, all of which have slew rates of about $5^\circ/\text{s}$ in azimuth and $1.2^\circ/\text{s}$ in elevation. In these simulations we only considered single telescopes at each site, although at several stations twin telescopes are planned or already exist. We generated an observing schedule with the VIE_SCHED software [9], applying the source-based scheduling strategy with four sources observed simultaneously. With this schedule, the very fast antennas made about 2000 scans/day, the others about 1600 scans/day. The schedule was repeated every sidereal day over the whole 25-day simulation period.

Simulated delays were generated with the VIE_SIM software [6]. First the theoretical delays were calculated, then we simulated random errors due to the clocks, the troposphere, and observation noise, and added these to the theoretical delays. For calculating the theoretical delay we used the observed EOP from a 25 days long period (4–29 September 2015). The clocks were simulated as random walk plus integrated random walk processes with an Allan standard devia-

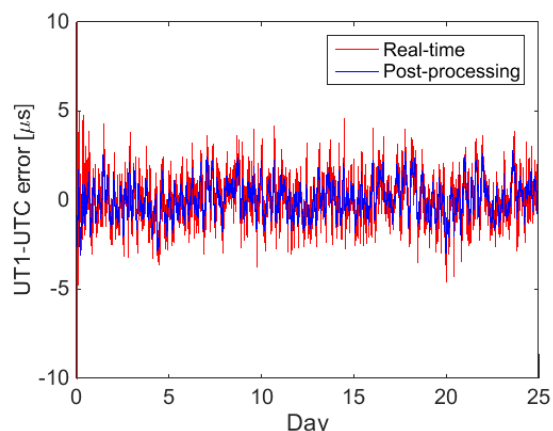


Fig. 3 The differences between the estimated UT1–UTC time series and the time series used as input to the simulations. Shown are both the results for real-time estimation and post-processing.

tion of $1 \cdot 10^{-14}$ @ 50 min, the tropospheric delay according to the algorithms presented in [3] with station specific C_n^2 values obtained from GPS data, and the observation noise was simulated as white noise with a standard deviation of 10 ps. The simulated delays were then used as input to the Kalman filter. As a priori EOP for the first epoch we used the actual EOP of this epoch plus random errors with standard deviations of 100 mas (polar motion), 2 ms (UT1–UTC), and 1 mas (celestial pole offsets). This represents very bad a priori EOP and was used in order to investigate how well the Kalman filter can deal with really poor a priori values.

4 Results

In Figure 3, the UT1–UTC values estimated from the Kalman filter are compared to the values used for creating the simulated delays. Two Kalman filter solutions were investigated: one real-time solution (only forward running Kalman filter) and one post-processed solution (forward and backward Kalman filter + smoothing). For the first epochs, there are large differences between the real-time estimates and the simulated values. The reason is that the a priori values used for the initial epoch contained large errors, thus the Kalman filter needs time in order to converge to the correct value. After a few hours, when the filter has converged, the precision of the estimates is more or less stable. Furthermore, we can see in Figure 3 that the scatter of the

Table 1 WRMS error in the EOP estimated in the real-time analysis and in post-processing.

	x-pole μas	y-pole μas	UT1–UTC μs	dX μas	dY μas
Real-time	27.7	24.6	1.29	20.6	21.3
Post-proc.	18.4	16.7	0.92	14.3	14.8

Table 2 WRMS error in the EOP estimated in the real-time analysis from the reduced data sets.

	x-pole μas	y-pole μas	UT1–UTC μs	dX μas	dY μas
10 stations	52.9	45.1	3.60	40.5	38.4
Every 5th scan	48.1	41.3	2.86	34.4	40.1
Every 10th scan	66.6	56.5	3.76	52.5	48.5

post-processed solution is lower than that of the real-time solution, as expected.

In Table 1 the Weighted Root-Mean-Square (WRMS) differences between the estimated and simulated EOP values are shown. We can see that the WRMS for the real-time estimates are about 40–50% larger than for the ones from the post-processing. A real-time estimate is only determined from the observations at the current and past epochs, while the post-processed estimate is determined also using future observations. Thus, we can say that the post-processed estimates are in principle determined from twice as many observations as the real-time ones. Based on this assumption, we would expect that the precision of the real-time estimates is about a factor of $\sqrt{2}$ worse than the post-processed ones, if we neglect correlations between the observables.

4.1 Reduced Data Set

In reality, it may be difficult to achieve real-time data transfer and correlation for a 30-station VGOS network. For example, some remote stations may not be connected to high-speed networks, or the correlator may not be able to receive all the data from all stations. One solution would be to only e-transfer part of the data, correlate this in real-time and use it to produce an ultra-rapid solution. The rest of the data is then sent later, e.g., by shipping disk modules, correlated, and then used to calculate the more accurate final solution. For example, the real-time e-transfer may be limited to only a few stations and/or selected scans.

We made tests where the real-time solution was calculated using only the observables from ten stations, every fifth scan, or every tenth scan. The WRMS differences between the estimated and simulated values are shown in Table 2. We can see that the WRMS values are much higher than those given in Table 1, as was to be expected due to the lower amount of data. It should be noted that no optimization was applied w.r.t. exactly which scans to include in the real-time solution. Thus, the results can be further improved by an optimal selection of the scans to e-transfer, e.g., instead of simply using scans number 1, 6, 11, and so on, one of the first five scans is chosen, then one of the next five scans, et cetera. Furthermore, it might be possible to make optimizations already in the scheduling w.r.t. the scans used in the real-time solution, although this might slightly degrade the final solution at the same time.

4.2 Clock Breaks and Other Problems

Occasionally, there are problems with the VLBI data, e.g., due to clock breaks. In the real-time analysis, these problems need to be automatically detected and corrected, otherwise the estimates would be affected. We have implemented automated clock break and outlier detection in the VieVS@GFZ real-time software. We make use of the fact that the Kalman filter makes predictions of the observed delays based on the estimates of the previous epoch. When the Kalman filter has converged, the difference between the observed and predicted delays can be expected to be small. Thus if there are large differences it may indicate a problem. It may, however, be difficult to directly determine the type of problem from the observations of just one scan. Thus, whenever large differences occur, we let the Kalman filter run without assimilating any data, i.e., only using predictions, for the next couple of epochs (the following 5 minutes) and compare the predictions at these epochs to the observed delays. If there is a clock break at one station, the difference between the predicted and observed delays will be large and of about the same size for all observations of this station. Hence, it is possible to detect the clock break and at which station it occurred. The clock break is then corrected by increasing the uncertainty of this clock's offset and rate in the Kalman filter; thus, more or less com-

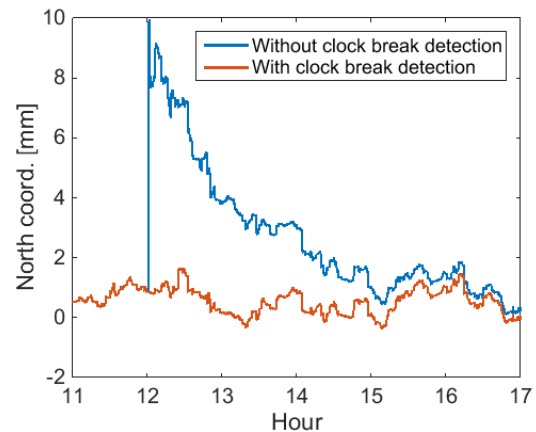


Fig. 4 The north coordinate estimates of the station with a clock break at 12:00. Shown are the results with and without using the automated clock break detection.

pletely new values will be estimated from the observations after the break. If large differences are present at one epoch but not at later epochs, it is an indication of an outlier; thus these observations are removed.

We tested the clock break detection by simulating a clock break of 0.66 ns (20 cm) at 12:00 UTC at one station. The software was able to detect and correct the clock break correctly. In Figure 4 we show the effect of this clock break on the north coordinate of this station. If the clock break detection and correction is not used, there is a jump in the coordinate of the station of almost 1 cm at the epoch of the clock break, and it takes several hours until the solution has converged back to the original level. On the other hand, if the automated clock break detection and correction is used, we see no effect on the north coordinate or any other estimated parameter.

5 Conclusions

Based on the real-time simulation results, the Kalman filter is able to estimate the polar motion and celestial pole offsets with a precision of 20–30 μas and UT1–UTC with a precision of 1.3 μs from a 30 station VGOS network. This is significantly better than what is obtained by the current VLBI system (about 100 μas for standard R1/R4 sessions, 30 μas for the CONT sessions [4]). However, the results are 40–50% worse compared to the results obtained in post-processing.

Thus it will still be beneficial to calculate a final solution with a delay of one or several days, in addition to the ultra-rapid real-time solution.

Acknowledgements

This work was supported by the Austrian Science Fund (FWF), project number P24187-N21 (VLBI-ART).

References

1. H. Hase, D. Behrend, A. Nothnagel, and H. Schuh. A vision for VGOS observations and analysis in 2020. In *Proceedings of the 22nd European VLBI Group for Geodesy and Astronomy Working Meeting*, pages 93–96, 2015. Available from: http://www.oan.es/raege/evga2015/EVGA2015_proceedings.pdf.
2. S. Matsuzaka, H. Shigematsu, S. Kurihara, M. Machida, K. Kokado, and D. Tanimoto. Ultra rapid UT1 experiment with e-VLBI. In A. Finkelstein and D. Behrend, editors, *Proceedings of the Fifth IVS General Meeting: Measuring the Future*, pages 68–71, 2008. Available from: <http://ivscc.gsfc.nasa.gov/publications/gm2008/>.
3. T. Nilsson and R. Haas. Impact of atmospheric turbulence on geodetic very long baseline interferometry. *J. Geophys. Res.*, 115:B03407, 2010. doi:10.1029/2009JB006579.
4. T. Nilsson, R. Heinkelmann, M. Karbon, V. Raposo-Pulido, B. Soja, and H. Schuh. Earth orientation parameters estimated from VLBI during the CONT11 campaign. *J. Geodesy*, 88(5):491–502, 2014. doi:10.1007/s00190-014-0700-5.
5. T. Nilsson, B. Soja, M. Karbon, R. Heinkelmann, and H. Schuh. Application of Kalman filtering in VLBI data analysis. *Earth Planets Space*, 67(136):1–9, 2015. doi:10.1186/s40623-015-0307-y.
6. A. Pany, J. Böhm, D. MacMillan, H. Schuh, T. Nilsson, and J. Wresnik. Monte Carlo simulations of the impact of troposphere, clock and measurement errors on the repeatability of VLBI positions. *J. Geodesy*, 85:39–50, 2011. doi:10.1007/s00190-010-0415-1.
7. B. Petrachenko, A. Niell, D. Behrend, B. Corey, J. Böhm, P. Charlot, A. Collioud, J. Gipson, R. Haas, T. Hobiger, Y. Koyama, D. MacMillan, Z. Malkin, T. Nilsson, A. Pany, G. Tuccari, A. Whitney, and J. Wresnik. Design aspects of the VLBI2010 system. In D. Behrend and K. Baver, editors, *International VLBI Service for Geodesy and Astrometry 2008 Annual Report*, NASA/TP-2009-214183. NASA Technical Publications, 2009.
8. B. Soja, T. Nilsson, M. Karbon, F. Zus, G. Dick, Z. Deng, J. Wickert, R. Heinkelmann, and H. Schuh. Tropospheric delay determination by Kalman filtering VLBI data. *Earth Planets Space*, 67(144):1–16, 2015. doi:10.1186/s40623-015-0293-0.
9. J. Sun, J. Böhm, T. Nilsson, H. Krásná, S. Böhm, and H. Schuh. New VLBI2010 scheduling strategies and implications on the terrestrial reference frames. *J. Geodesy*, 88(5):449–461, 2014. doi:10.1007/s00190-014-0697-9.